Earthquakes and Structures, *Vol. 5, No. 5 (2013) 499-526*
DOI: http://dx.doi.org/10.12989/eas.2013.5.5.499

Assessing the effect of inherent nonlinearities in the analysis and design of a low-rise base isolated steel building

Varnavas Varnava[a] and Petros Komodromos[*]

Department of Civil and Environmental Engineering, University of Cyprus, Nicosia, 1687, Cyprus

(Received November 20, 2012, Revised April 28, 2013, Accepted July 15, 2013)

Abstract. Seismic isolation is an effective method for the protection of buildings and their contents during strong earthquakes. This research work aims to assess the appropriateness of the linear and nonlinear models that can be used in the analysis of typical low-rise base isolated steel buildings, taking into account the inherent nonlinearities of the isolation system as well as the potential nonlinearities of the superstructure in case of strong ground motions. The accuracy of the linearization of the isolator properties according to Eurocode 8 is evaluated comparatively with the corresponding response that can be obtained through the nonlinear hysteretic Bouc-Wen constitutive model. The suitability of the linearized model in the determination of the size of the required seismic gap is assessed, under various earthquake intensities, considering relevant methods that are provided by building codes. Furthermore, the validity of the common assumption of elastic behavior for the superstructure is explored and the alteration of the structural response due to the inelastic deformations of the superstructure as a consequence of potential collision to the restraining moat wall is studied. The usage of a nonlinear model for the isolation system is found to be necessary in order to achieve a sufficiently accurate assessment of the structural response and a reliable estimation of the required width of the provided seismic gap. Moreover, the simulations reveal that the superstructure's inelasticity should be taken into account, especially if the response of the structure under high magnitude earthquakes is investigated. The consideration of the inelasticity of the superstructure is also recommended in studies of structural collision of seismically isolated structures to the surrounding moat wall, since it affects the response.

Keywords: seismic isolation; base isolation; rubber bearings; Bouc-Wen model; seismic gap; nonlinear analysis; superstructure's inelasticity; collision to moat wall

1. Introduction

Base or seismic isolation is an innovative design approach, used for the minimization of earthquake induced loads and the avoidance of damage in relatively stiff buildings. The method is based on the decoupling of a structure from the horizontal components of ground motions, by the insertion of flexibility at the isolation level, and the avoidance of resonance, as the fundamental frequencies of the structure are shifted away from the predominant frequencies range of common earthquakes. The interstory deflections, floor accelerations and shear forces can be significantly

[*]Corresponding author, Assistant Professor, E-mail: komodromos@ucy.ac.cy
[a] Ph.D. student, E-mail: varnavas@logosnet.cy.net

 ISSN: 2092-7614 (Print), 2092-7622 (Online)

reduced, while structural and non-structural damage can be avoided (Naeim and Kelly 1999, Komodromos 2000). The two main categories of seismic isolation systems are the elastomeric bearings and the friction-sliding systems. The elastomeric bearings can be subdivided in the Natural Rubber Bearings (NRBs), the High Damping Rubber Bearings (HDRBs) and the Lead Rubber Bearings (LRBs) (Higashino and Okamoto 2006). The NRBs provide necessary horizontal stiffness to the structure, but their energy dissipation capacity is usually insufficient, since their damping is limited in the 2-3 % range of the critical viscous damping (Kelly 2001). Thus, NRBs are generally used in combination either with HDRBs or LRBs, or with additional damping devices, necessary for the provision of adequate supplemental damping to the structure in order to suppress the expected large relative displacements at the isolation level.

The primary aim of this paper is the evaluation of the suitability of the linear and nonlinear models that can be used in the analysis of typical low-rise base isolated buildings, considering nonlinearities of these buildings at both the isolation system and the superstructure. This research works focuses on the seismic response of a two story steel structure, equipped with a hybrid isolation system that consists of NRBs and LRBs. The NRBs are characterized by an essentially linear behavior and a viscous damping mechanism (Skinner *et al.* 1993), while the LRBs exhibit a non-linear hysteretic behavior. The linearization of the LRBs' behavior, which is allowed by Eurocode 8, under certain conditions, is not always an adequately accurate approach (Mavronicola and Komodromos 2011). In order to evaluate the accuracy of the linearization of the LRBs' properties, three-dimensional (3D) non-linear time-history analyses are performed, using the nonlinear hysteretic Bouc-Wen constitutive model. Moreover, the simulated base isolated structure is subjected to higher magnitude earthquakes than the design basis earthquake (DBE), so as to determine the size of the required seismic gap and assess the appropriateness of the proposed, by the Eurocode 8 and the Uniform Building Code 1997 (UBC 1997), methods for the preliminary calculation of the width of the required seismic gap.

Furthermore, in most research studies of seismically isolated buildings, the behavior of the superstructure is assumed linear elastic. The validity of this assumption, which comprises a provision of Eurocode 8, is also investigated under various earthquake magnitudes and the alteration of the response due to the inelastic deformations of the superstructure is explored. Additionally, the structural failures are compared with those obtained from the analyses of models with linear elastic behavior of the superstructure.

Finally, since seismically isolated buildings experience relatively large displacements at the isolation level, especially during high magnitude earthquake excitations with strong low frequency content, the seismic response of the building when collision incidents with a surrounding moat wall take place has also been considered. It is a "common practice" that the behavior of the superstructure of the buildings is considered linear elastic, assuming that the structural response during collisions to a restraining moat wall is mainly governed by the isolation system's response. The particular investigation focuses on the quantification of the structural response's shift due to the inelastic deformations of the superstructure.

2. Research objectives and scope

2.1 Shear behavior and modeling of lead rubber bearings

The nonlinear hysteretic shear behavior of LRBs can be described by an inelastic bilinear model, characterized by the high initial elastic stiffness, K_{el}, the low post-yield stiffness, K_{py}, the yield

force and displacement, F_y and U_y, respectively, the characteristic strength, Q, and the maximum force and displacement, F_D and U_D, respectively (Fig. 1). Although the bilinear model describes sufficiently well the accuracy of the shear behavior of LRBs, it incorporates a sudden transition from the elastic to the post elastic branch. The Bouc-Wen model, proposed by Bouc (1967), elaborated by Wen (1976), modified by Park *et al.* (1986) and recommended for base isolation analysis by Nagarajaiah et al (1991), ensures a smooth transition between the two branches, as it is shown by the dashed curves in Fig. 1, has been implemented in various engineering applications (Charalampakis and Koumousis 2008) and is commonly used for the simulation of LRBs' behavior (Wu *et al.* 2008, Providakis 2008).

The hysteretic behavior of the Bouc-Wen model is expressed by a single equation regardless the state of the nonlinear response. The nonlinear restoring force for a SDOF system takes the form of Eq. (1). This equation describes the action of two springs connected in parallel, one elastic post-yield spring and one hysteretic spring. The internal hysteretic variable *z(t)* is described by a nonlinear differential equation (Eq. (2)).

$$F(t) = F^{pel} + F^{h} = r \cdot K_{el} \cdot u(t) + (1 - r) \cdot F_y \cdot z(t) \tag{1}$$

Where:

$u(t)$: Horizontal displacement as a function of time

r : Ratio of the post-yield stiffness K_{py} to the elastic stiffness K_{el}

$z(t)$: Internal dimensionless hysteretic variable, $|z(t)| \le 1$

$$\dot{z}(t) = \frac{1}{u_y} \cdot \left[A - |z(t)|^n \cdot (\beta + sign(\dot{u}(t) \cdot z(t)) \cdot \gamma) \right] \cdot \dot{u}(t) \tag{2}$$

In the particular problem, where the spatial seismic response of a 3D model is investigated, the isolators are subjected to biaxial shear forces. So, the Bouc-Wen model behavior is considered for the two horizontal translational degrees of freedom, x and y, of each LRB (Eq. (3) & Eq. (4)) in terms of the above parameters in the x and y. The biaxial shear inelastic behavior of these isolators is coupled and the evolvement of the deformations of the two aforementioned degrees of freedom is expressed through two differential equations, which are represented by Eq. (5), and implemented in SAP2000 v.15.

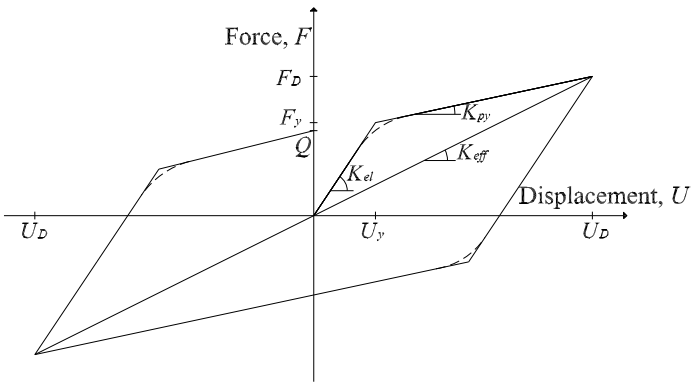

Fig. 1 Inelastic shear behavior constitutive law of a LRB

$$F_x(t) = r_x \cdot K_{el-x} \cdot u_x(t) + (1 - r_x) \cdot F_{y-x} \cdot z_x(t) \tag{3}$$

$$F_y(t) = r_y \cdot K_{el-y} \cdot u_y(t) + (1 - r_y) \cdot F_{y-y} \cdot z_y(t) \tag{4}$$

$$\begin{Bmatrix} \dot{z}_x(t) \\ \dot{z}_y(t) \end{Bmatrix} = \begin{bmatrix} 1 - \alpha_x \cdot [z_x(t)]^2 & -\alpha_y \cdot z_x(t) \cdot z_y(t) \\ -\alpha_x \cdot z_x(t) \cdot z_y(t) & 1 - \alpha_y \cdot [z_y(t)]^2 \end{bmatrix} \cdot \begin{Bmatrix} \frac{K_{el-x}}{F_{y-x}} \cdot \dot{u}_x(t) \\ \frac{K_{el-y}}{F_{y-y}} \cdot \dot{u}_y(t) \end{Bmatrix} \tag{5}$$

$$\sqrt{[z_x(t)]^2 + [z_y(t)]^2} \leq 1 \tag{6}$$

Where the parameters α_x and α_y are provided by the following expressions

$$\alpha_x = \begin{cases} 1, \text{ if } u_x(t) \cdot z_x(t) > 0 \\ 0, \text{ in the rest cases} \end{cases}$$

$$\alpha_y = \begin{cases} 1, \alpha\nu \ \dot{u}_y(t) \cdot z_y(t) > 0 \\ 0, \text{ in the rest cases} \end{cases}$$

In practice, equivalent linear elastic models are often used in order to further simplify the design and analysis of seismically isolated buildings, at least at the preliminary design and analysis phases. According to Eurocode 8, the seismic isolation system, under certain limitations, can be modeled assuming an equivalent linear viscoelastic behavior, based on an effective stiffness, K_{eff}, and an effective viscous damping ratio, ξ_{eff}, of the isolation system (Eq. (7) & Eq. (8)). Thus, it is very important to investigate the appropriateness of using such a linearized model, by comparing its computed responses with those of the more accurate Bouc-Wen model. Eq. (9) and Eq. (10) are used to derive expressions for the calculation of the effective stiffness, $K_{effisol}$, and the effective viscous damping ratio, $\xi_{effisol}$, of the isolation system, since the isolation system under consideration is composed of both LRBs and NRBs.

$$K_{eff} = K_{py} + \frac{Q}{U_D} \tag{7}$$

$$\xi_{eff} = \frac{4 \cdot Q \cdot (U_D - U_y)}{2 \cdot \pi \cdot K_{eff} \cdot U_D^2} \tag{8}$$

$$K_{effisol} = \sum_{i=1}^{n} K_{effNRBi} + \sum_{j=1}^{m} K_{effLRBj} = \sum_{i=1}^{n} K_{rbi} + \sum_{j=1}^{m} \left(K_{pyj} + \frac{Q_j}{U_{Dj}} \right) \tag{9}$$

$$\xi_{effisol} = \frac{W_{DLRBs} + W_{DNRBs}}{2 \cdot \pi \cdot K_{effisol} \cdot U_D^2} = \frac{4 \cdot \left(\sum_{j=1}^{m} Q_j \right) \cdot (U_D - U_y) + 2 \cdot \pi \cdot \left(\sum_{i=1}^{n} K_{rbi} \right) \cdot \xi_{effNRB} \cdot U_D^2}{2 \cdot \pi \cdot K_{effisol} \cdot U_D^2} \quad (10)$$

Where:

$K_{effNRBi}$, $K_{effLRBi}$:	Effective stiffness of a NRB and a LRB isolator, respectively
K_{rbi}:	Rubber stiffness of a NRB isolator
n, m:	Number of NRB and LRB isolators respectively
W_{DNRBs}, W_{DLRBs}:	Energy dissipated through a loading, unloading and reloading cycle, from the NRBs and the LRBs, respectively
ξ_{effNRB}:	Equivalent viscous damping ratio of a NRB isolator (≈2 %)

Iwan and Gates (1979) studied the response of six hysteretic bilinear models in comparison with the response of the respective linearized models, through numerical simulations. They concluded that the linearized models provide relatively accurate estimation of the response for moderate values of eigenperiods. In addition, they observed that the usage of the effective viscous damping ratio results in the overestimation of the hysteretic energy dissipation of the system. Matsagar and Jangid (2004) analyzed the influence of isolator characteristics on the seismic response of base isolated structures modeled as MDOF, suggesting that equivalent linear elastic models mainly underestimate the accelerations of the superstructure and overestimate the maximum relative displacements of the isolators. They also underlined the substantial effect of the excitations' frequency content and the isolators' eigenperiod and damping in the structural response. Dicleli and Buddaram (2007) evaluated the linearization of the shear behavior of elastomeric and other bearings, concluding that the linearized model underpredicted the isolators' maximum displacements and developed forces. Mavronicola and Komodromos (2011) investigated the appropriateness of various literature-proposed relationships for the linearization of stiffness and the conversion of hysteretic to equivalent viscous damping of LRBs, concluding that usage of the proposed relationships results in overestimation of the maximum relative displacements at the isolation level and leads to large response discrepancies in comparison with those computed by the more accurate bilinear model. Makris and Kampas (2013) investigated the accuracy of the effective period approach for several bilinear isolation systems, by employing Fourier and Wavelet analysis together with a time domain identification method, named Prediction Error Method. They concluded that the linearization of the vibration period of these systems has a marginal engineering merit, since the systems' response is dominated by the nonlinear behavior of the isolation system. Moreover, they developed a matching index that can be applied for the selection of the "proper" response histories where the concept of associating a vibration period is meaningful.

2.2 Determination of the required width of the seismic gap

Between a seismically isolated structure and the surrounding structures a sufficient clearance, known as seismic gap, should be provided in order to accommodate the large horizontal relative displacements that are expected at the isolation level. Chapter 10 of Eurocode 8-1 provides a

methodology for the calculation of the required seismic gap, which takes explicitly into account the accidental torsional displacements of the isolation system. Moreover, Appendix Chapter 16 of UBC 1997 states that the total design displacement and the total maximum displacement, thus the peak displacement under the maximum credible earthquake, should comprise the additional displacement due to actual and accidental torsion. The appropriateness of the methodologies of the two design codes is assessed in comparison with the calculated displacements derived from both linear and nonlinear analyses, for three different levels of peak ground acceleration (PGA) of the imposed earthquake excitations.

2.3 Superstructure's inelastic behavior

The superstructure of a seismically isolated building is designed to remain in the elastic range under earthquake excitations with magnitude equal to the DBE. However, it is important to explore potential failures and their mechanisms, under stronger excitations than the DBE and investigate their influence on the structural response. Providakis (2008) studied the inelastic response of two composite, seismically isolated structures - one moment resisting frame and one braced frame with concentric braces – through a pushover analysis, using a concentrated inelasticity approach to consider the inelastic behavior of the columns and the beams but without considering the potential inelastic deformations of the braces. The moment resisting frame developed inelastic deformations up to the 4^{th} story, while the introduction of the braces limited them up to the 2^{nd} story. Kilar and Koren (2010) investigated the inelastic response of a seismically isolated concrete structure with pushover and nonlinear time-history analyses. They concluded that the assumption of linear elastic behavior for the superstructure results in the underprediction of interstory deflections and in the overprediction of the displacements of the isolation system, even under excitations of the same magnitude with the DBE. Cardone et al (2011) explored the inelastic response of the superstructure of the seismically isolated buildings, by subjecting two degree of freedom systems, isolated with HDRBs, LRBs and friction pendulum systems (FPSs), to nonlinear time-history analyses. They observed that the increase of the LRBs damping ratio resulted in an increase of the superstructure's ductility demand, whereas the increase of HDRBs damping ratio lead to a reduction of the superstructure's ductility demand. Another important observation was that the superstructure's inelastic deformations had negligible effect on the response of the isolation system.

2.4 Potential poundings with the surrounding moat wall

The seismically isolated building under consideration develops large relative displacements at the isolation level, a fact that makes possible a collision with the surrounding moat wall. Although the seismic performance of base isolated structures considering potential structural pounding has been explored by a few researchers, most relevant studies are based on very minimal, macroscopic models, such as stick models, that cannot take into account details at a structural element level or any spatial effects. The current study investigates the discrepancies in the response of a seismically isolated building pounding against the surrounding moat wall, if linear elastic or explicit inelastic behavior of the superstructure is considered.

The first analytical investigation of pounding of seismically isolated buildings against a moat wall is credited to Tsai (1997). In that study, the analyses were based on a wave propagation theory, modeling the isolation system as either linearly elastic or elastoplastic and the superstructure as a

shear beam with either viscoelastic or elastoplastic behavior. The results indicated that the sudden change of the stiffness at the base of the shear beam created impact waves that travelled along the beam and induced an extremely high acceleration response in the shear beam, especially when the latter remained elastic. If the shear beam yielded during excitation, the impact waves could not propagate through the shear beam and only the base of the shear beam was subjected to high accelerations.

Mahmoud and Jankowski (2010) investigated numerically the seismic response of adjacent fixed-base and seismically isolated buildings considering impacts between bases and superstructures by simulating the buildings using elastoplastic lumped mass models. They concluded that in the case of a seismically isolated building colliding with either a seismically isolated or a fixed-base building, the variation of the stories' responses is relatively low while significant discrepancies were noted in the case of a fixed-base building colliding with an either a seismically isolated or a fixed-base building. Pant and Wijeyewickrema (2012) studied the structural performance of a base isolated reinforced concrete building colliding either with an identical conventionally based building or with retaining walls. Their analyses revealed that the lower stories of the base isolated building were most vulnerable when pounding with the retaining wall was considered, whereas upper stories developed more damage compared with lower stories when bilateral pounding with the retaining wall and the fixed-base building was considered.

Since pounding of a seismically isolated building with a moat wall induces catastrophic consequences, Polycarpou and Komodromos (2011) recommended the insertion of rubber bumpers at locations where it is likely to have impacts. The incorporation of these elements, which act as shock absorbers, was found to be effective, especially for relatively narrow seismic gaps, since they resulted in the elongation of the impact duration and in the reduction of the high spikes in the acceleration response.

3. Structural modeling

3.1 Description of structure

The building under consideration is a 2 story dwelling located in a region in Cyprus, where the design ground acceleration is 0.25 g and the foundation soil is type B, according to Eurocode 8. The members of the superstructure are made of hot-rolled steel, grade S275, and the floor slabs are composite with high-strength trapezoidal steel sheets. The building is regular in plan and elevation, with 24 m x 20 m plan dimensions and 3.3 m story height. The lateral force resisting system in the principal *X*-direction is a moment resisting frame. As shown in Fig. 2, the structural system of the outer frames in the secondary *Y*-direction consists of a plain frame with pin-based columns and pin-ended tie beams. The outer frames in the *Y*-direction are equipped with x-diagonal braces on the edge bays. For the design of the hybrid isolation system, consisting of 14 NRBs and 6 LRBs, a target fundamental period, T_{dtar}, of 1.20 sec and an effective viscous damping ratio of 15 % have been assumed. A detailed design procedure has been applied, which incorporated the design of each isolator type (determination of the stiffness and damping), the capacity checks (vertical load bearing capacity, critical buckling load) and the derivation of the characteristics of the isolation system. The main geometrical properties and the mechanical characteristics of each type of isolator are provided in Table 1.

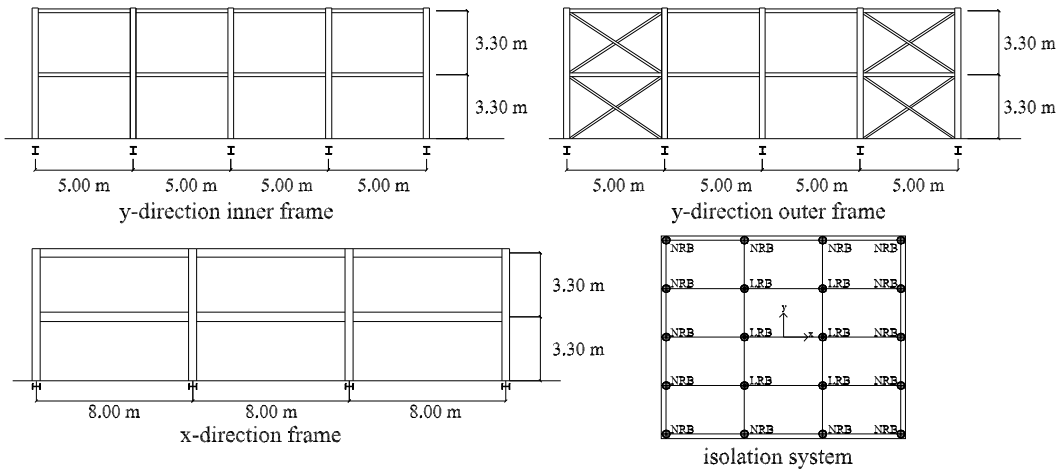

Fig. 2 Structural and seismic isolation systems

Table 1 Characteristics of seismic isolators

Bearing	NRB	LRB
1. Geometrical Properties		
Outer diameter (mm)	510	510
Elastomeric layer diameter (mm)	460	460
Elastomeric layer thickness (mm)	10	10
Number of elastomeric layers	10	10
Isolator total height (mm)	160	160
Lead core diameter (mm)	-	82.5
Shape factor	11.50	11.13
2. Mechanical Characteristics		
Isolator mass (kg)	111.60	117.30
Design displacement (mm)	94.90	94.90
Yield displacement (mm)	-	2.708
Initial elastic shear stiffness (MN/m)	0.6648	20.3835
Post-yield stiffness (MN/m)	-	0.6434
Total axial stiffness (MN/m)	722.46	509.73
Torsional stiffness (kNm)	12.4330	12.4201
Characteristic strength (kN)	-	53.4562
Critical buckling load (kN)	6835.40	6504.85
Effective damping coefficient (kNsec/m)	5.01	161.07

3.2 Modeling of the isolation system

The isolators are modeled by utilizing hysteretic rubber isolator link elements, which are incorporated in SAP2000. Linear elastic properties, determined for each studied level of the excitations' PGA, are defined for the NRBs' horizontal, translational degrees of freedom. Also, linearized properties are assigned to the respective degrees of freedom of the LRBs of the linear model (LM). The energy dissipation capacity of the seismic isolation system is expressed through an equivalent viscous damping ratio, introduced into the Rayleigh damping matrix. Nonlinear

properties, according to the Bouc-Wen model, are defined for the LRBs' nonlinear models (NLM). Values 1.0, 0.5, 0.5 and 2 are adopted for the Bouc-Wen models' parameters A, β, γ and n respectively, which are suggested by Chen *et al.* (2006) and Qiang *et al.* (2010) in relevant studies.

3.3 Modeling of the superstructure

The inelasticity of all potentially inelastic deformable structural elements is simulated in terms of an extended nonlinear model (ENLM). The main beams of the superstructure develop significant moment about their strong axis and relatively low shear force, which does not induce inelastic deformation. Concentrated inelasticity elements, thus inelastic uniaxial bending hinges, are assigned at the end of the beams and the respective moment-rotation relationship is determined according to the provisions of FEMA 356 (Fig. 3).

The braces of the building are axially stressed, so the potential inelastic deformations are caused due to tension or axial buckling. One inelastic axial hinge is assigned at the midpoint of every brace, which is the point at which buckling initiates (Fig. 3). The axial force-deformation relationship that has the same pattern for tensile and buckling deformations, but different inelastic deformation capacities, is also derived according to FEMA 356. Beyond yield, the assigned inelastic hinges simulate phenomena such as ultimate capacity, strength loss and complete failure. The hardening behavior of the hinges is described by a kinematic hardening type, which is recommended by Powel (2010) since it is more conservative than isotropic hardening. The critical modes of failure of the columns are compression and bending about their strong and weak axes, as well as the interactions of the aforementioned internal forces. Instead of assigning discrete inelastic hinges for each potential mode of failure, the implementation of fiber elements, which is suggested by Elnashai and Di Sarno (2008), is deemed more practical, since a single fiber zone can capture all these phenomena and simulates more accurately the axial force-biaxial moment interaction. The implementation of fiber hinges is considered redundant for the particular beams, which are characterized by only one potential mode of yield, since it would result in a dramatic increase of the computational cost without any worthy contribution to the accuracy of the results.

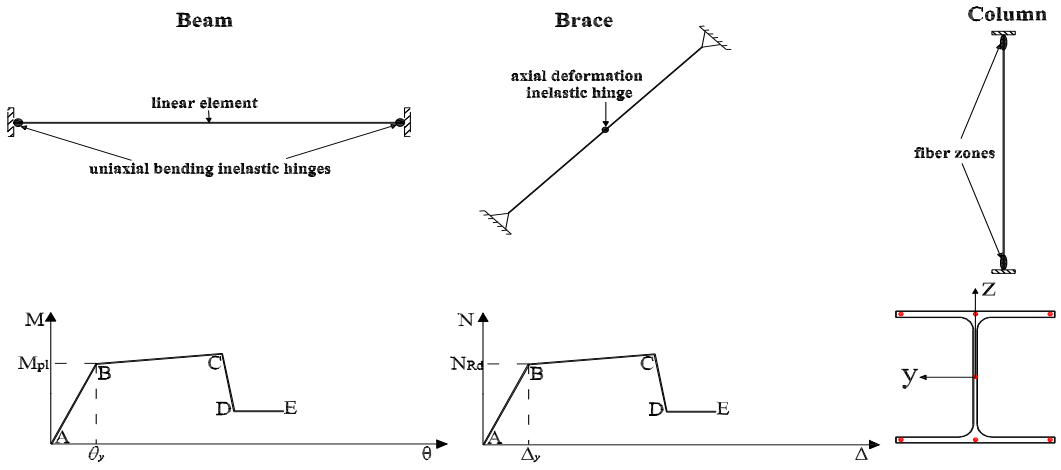

Fig. 3 Modeling of the inelastic behavior of structural elements

3.4 Modeling of potential collision of the building against the restraining moat wall

Collision phenomena along the two principal, horizontal directions of the seismically isolated structure are also investigated. The detection of impact is performed with the assignment of gap elements at the potential points of collision with the adjacent rigid moat wall (Fig. 4). The behavior of a gap element is described by Eq. (11). The impact stiffness is represented by k_{imp}, variable *open* determines the initial distance between the colliding structures, while variable d represents the deformation of the gap element. It is obvious from this equation that the gap elements are activated only when collision occurs. Since, this study focuses on the alteration of the response of a seismically isolated building due to the inelastic deformations of the superstructure; collisions are investigated under a higher level of PGA, 0.50 g, which can induce more intensive inelastic response. For the same reason, for each seismic combination, the initial distance between the colliding structures is defined as the half of the maximum unobstructed displacement at the seismic isolation level under the respective unhampered oscillation. The impact stiffness is obtained through a thorough parametric analysis.

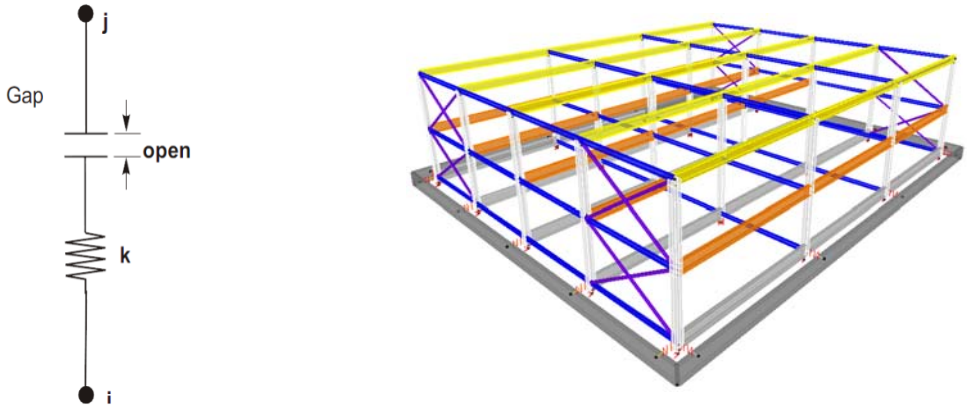

Fig. 4 Arrangement of gap elements

$$f = \begin{cases} k_{imp} \cdot (d + open) & \text{if } d + open < 0 \\ 0 \text{ if } & d + open \geq 0 \end{cases} \tag{11}$$

4. Methodology

Seven pairs of accelerograms, consisting of the X and Y components of strong earthquake excitations (Table 2), are selected for the time-history analyses of the seismically isolated structure (SIS), which are performed using SAP2000. The acceleration response spectrum of the adopted earthquake records, scaled to the design ground acceleration on type A ground (0.25 g) are

Table 2 Earthquake ground motions

Earthquake	Date	Station	Components
Kalamata	13/09/1986	OTE- Building	N10W / N80E
Athens	07/09/1999	Sepolia (Garage)	LONG / TRAN
Ionian	04/11/1973	Lefkada OTE- Building	E-W / N-S
Thessalonika	20/06/1978	Thessaloniki-City Hotel	E-W / N-S
Kocaeli	17/08/1999	Duzce-Meteoroloji Mudurlugu	SN / WEST
Northridge	17/01/1994	Sylmar - County Hospital Parking Lot	1:90 Deg / 3:360 Deg
Parkfield	27/06/1966	Cholame Shandon	N85E / N05W

Table 3 Load combinations

Load Combination	Combined Actions	Limit State
LC_1:	$1.00G + 1.00Q$	Serviceability
LC_2:	$1.35G + 1.50Q$	Ultimate
EC_1:	$1.00G + 0.30Q+1.00E_x+0.30E_y$	Ultimate
EC_2:	$1.00G + 0.30Q+0.30E_x+1.00E_y$	Ultimate

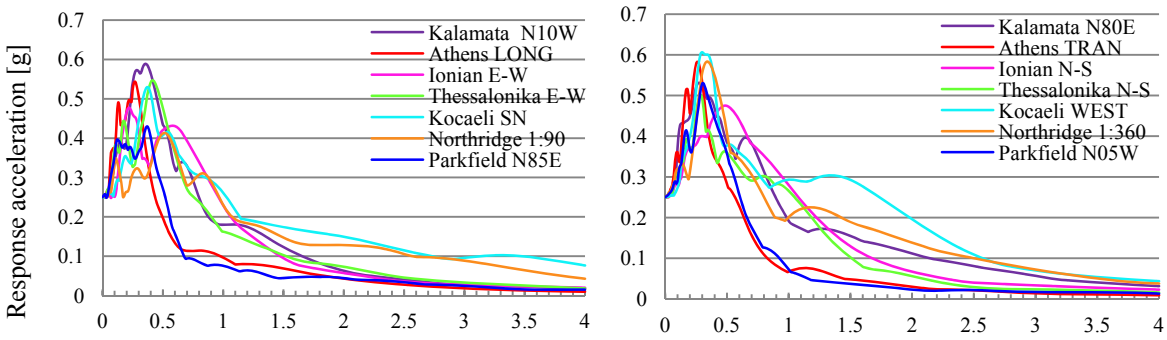

(a) (b)

Fig. 5 Acceleration response spectrums of the considered earthquake excitations along the (a) *X* direction and (b) the *Y* direction

represented in Fig. 5. The accelerograms are scaled for 3 levels of PGA: 0.30, 0.40 and 0.50 g. The two higher levels of PGA correspond to severe earthquake excitations, such as the maximum credible earthquake. Four load patterns are considered, the dead load, G, the live load, Q, the earthquake action along the X direction, E_x, and the earthquake action along the Y direction, E_y, while the structural response is obtained for 4 load combinations; one for the serviceability limit state and three for the ultimate limit state (Table 3).

The differential equations of motion are solved using the Newmark (β=0.25, γ=0.50) direct time-integration method. The analysis and design of the SIS is performed simultaneously with the analysis and design of an identical conventionally based structure (CBS), for comparison purposes. The two structures are designed so as to respond elastically under all the imposed earthquake

excitations, scaled to a PGA equal to 0.30 g, while a common performance level is set, specifically, the equal maximum relative displacement of their first story. Identification of failures and structural optimization in models with linear elastic behavior of the superstructure is carried out by performing design checks, according to the provisions of Eurocode 3, which are incorporated in SAP2000.

The insertion of the isolation system shifts the fundamental period of the building from 0.212 to 1.292 sec. Since the ratio of the fundamental period of the SIS to the fundamental period of the conventionally based structure (CBS) is greater than 3, the torsional amplifications are limited and the ductility demand of the corner isolators is reduced (Tena-Colunga and Escamilla-Cruz, 2007). Also, the torsional to lateral frequency ratio, as defined in Kilar and Koren (2009), is greater than unity, which indicates that the SIS is torsionally restrained. Fig. 6 provides the first 3 mode shapes of the SIS and the CBS, while Table 4 provides the corresponding modal participation factors, indicating the increased contribution of the predominant modes in the overall response of the SIS,

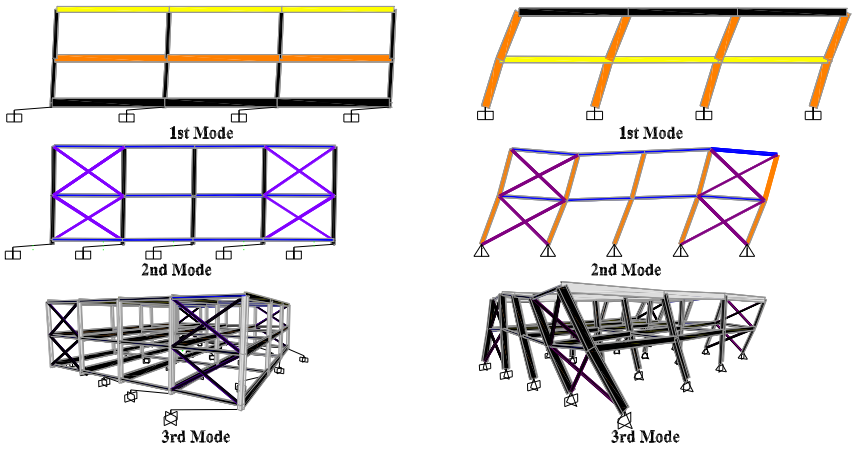

Fig. 6 Fundamental eigenmodes of the SIS and CBS

Table 4 Fundamental eigenperiods and participation factors of the CBS and SIS

	Mode	Period (sec)	Modal Participating Mass Ratios		
			U_x (%)	U_y (%)	R_z (%)
CBS	1	0.212	85.2	0	24.5
	2	0.151	0	93.0	38.5
	3	0.116	0	0	27.2
SIS	1	1.292	99.8	0	28.9
	2	1.267	0	100.0	41.7
	3	1.221	0	0	29.3

whereas higher modes participate in the oscillation of the CBS. While base isolation minimizes the interstory deflections due to the almost rigid body motion of the superstructure, the lateral load resisting system of the CBS had to be strengthened in order to reduce the interstory deflections to targeted levels. For this reason, HEB 600 and CHS 168.3x12.5 are used for the CBS column sections and brace sections, respectively, instead of HEA 300 and CHS 139.7x5, which are used for the SIS. Moreover, HEA 450 and IPE 550 are used for the major beams of the first and second story, respectively, of the CBS, while IPE 500 and IPE 400 are used for the SIS.

5. Evaluation of the accuracy of the linearized constitutive law of the LRBs

The use of the Bouc-Wen constitutive law for modeling the LRBs' shear behavior has a rather insignificant effect on the envelope of the maximum displacements of the specific isolation system along the two principal horizontal directions (Fig. 7(a)). However, the linearization of the LRBs' behavior affects strongly the maximum interstory deflections, as it can be noticed in Fig. 7(b). The maximum interstory deflections of stories 1 and 2, along the *X* direction, are insecurely underestimated by 13.9 and 23.5 %, respectively, and the corresponding relative error increases substantially with height. Contrarily, the maximum interstory deflections of stories 1 and 2, along the *Y* direction, are overestimated by 10.8 and 11.5 %, respectively. This corresponding variation of the relative error indicates that the characteristics of the superstructure and specifically its stiffness as well as the frequency content of the earthquake excitations influence the accuracy of the LRBs' linearized shear behavior.

It is evident from Fig. 8, that the linear model estimates sufficiently well the maximum relative displacements of the isolation system, under earthquake excitations that cause relatively intensive response of the structure. This is due to the fact that the maximum displacements developed at the isolation level are similar with the horizontal design displacement of the isolation system, which is approximately 7.9 cm. However, the use of the linearized model leads to significant overestimation of the isolation system's displacements, under earthquake excitations that cause moderate structural response. The substantial error, which is obvious in Fig. 9, is related to the linearization methodology of the isolators' shear behavior. Specifically, the effective shear stiffness of the

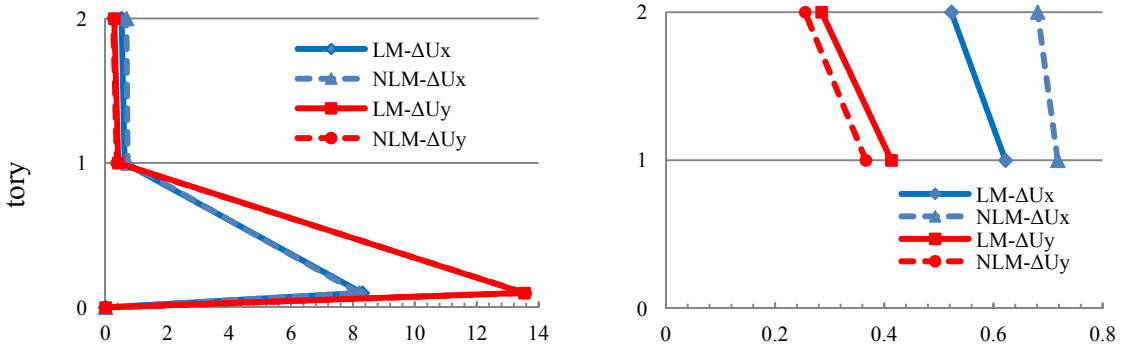

(a) Structure's deflections [cm] (b) Superstructure's deflections [cm]

Fig. 7 Envelope of maximum (a) structure's interstory deflections and (b) superstructure's interstory deflections, along the X and Y directions under the EC_1 and EC_2 combinations, respectively

isolators, K_{eff}, which is determined based on the horizontal design displacement of the isolation system, is much lower than their actual stiffness under low or moderate displacements, as it is represented by $K_{act\text{-}l}$ and $K_{act\text{-}m}$ dashed red lines in Fig. 10, resulting in unrealistically higher displacements.

Furthermore, as it is shown in Fig. 11, under certain excitations, which cause moderate structural response, the linearized model tends to yield non-conservative underestimations of the interstory deflections of the superstructure. The effective viscous damping ratio, which is calculated according to the design displacement, is higher than the actual value, since the area of the actual hysteretic loops is less than the area of the loop at the design displacement. Thus, the ad

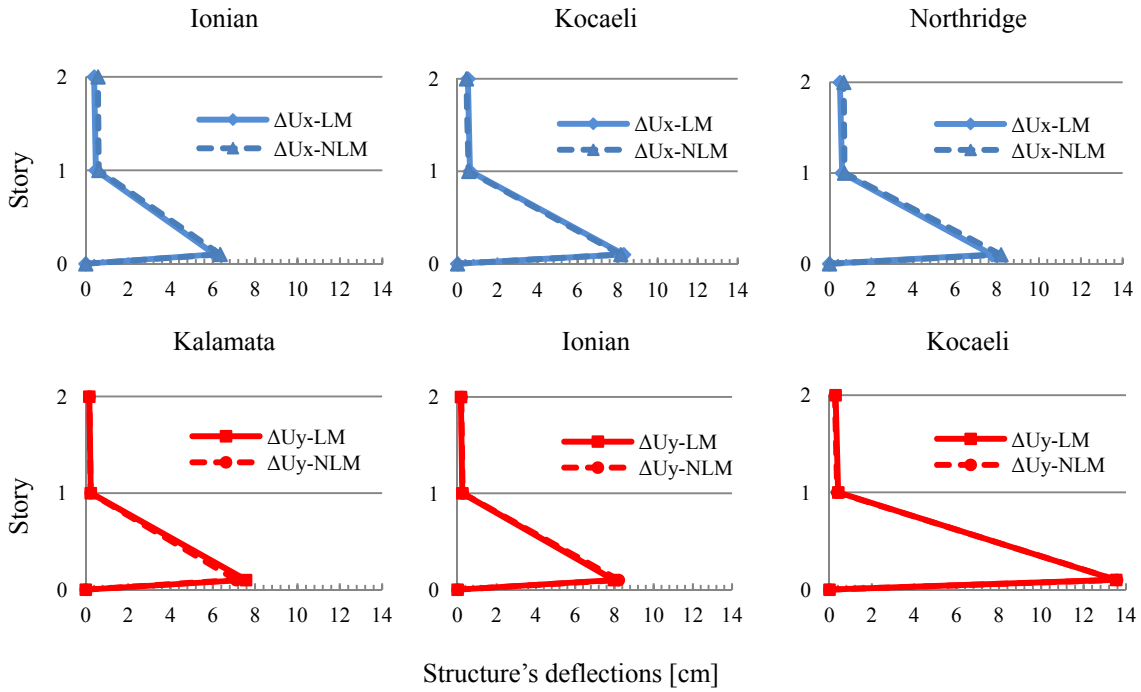

Fig. 8 Interstory deflections under earthquake excitations that cause intensive structural response

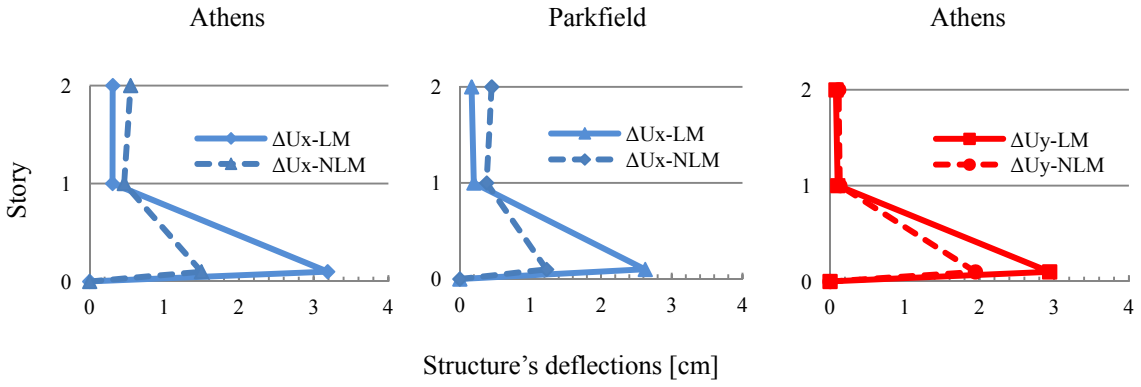

Fig. 9 Interstory deflections under earthquake excitations that cause moderate structural response

hoc overestimated effective damping reduces the interstory deflections. It is also noteworthy, that along the *X* direction, under certain excitations, the usage of linear analysis results in reduction of the interstory deflections with height, while the interstory deflections computed by the more accurate nonlinear model are amplified with height (Fig. 11). Besides the overestimated effective damping of the isolation system, its underestimated effective stiffness and, consequently, the overestimated fundamental eigenperiod result in a reduction of the earthquake induced loads, leading to the computation of non-conservative interstory deflections.

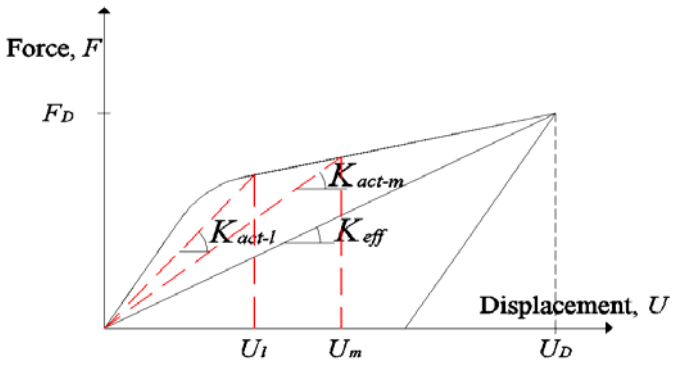

Fig. 10 Effective and actual shear stiffness of the isolators under low and moderate displacements

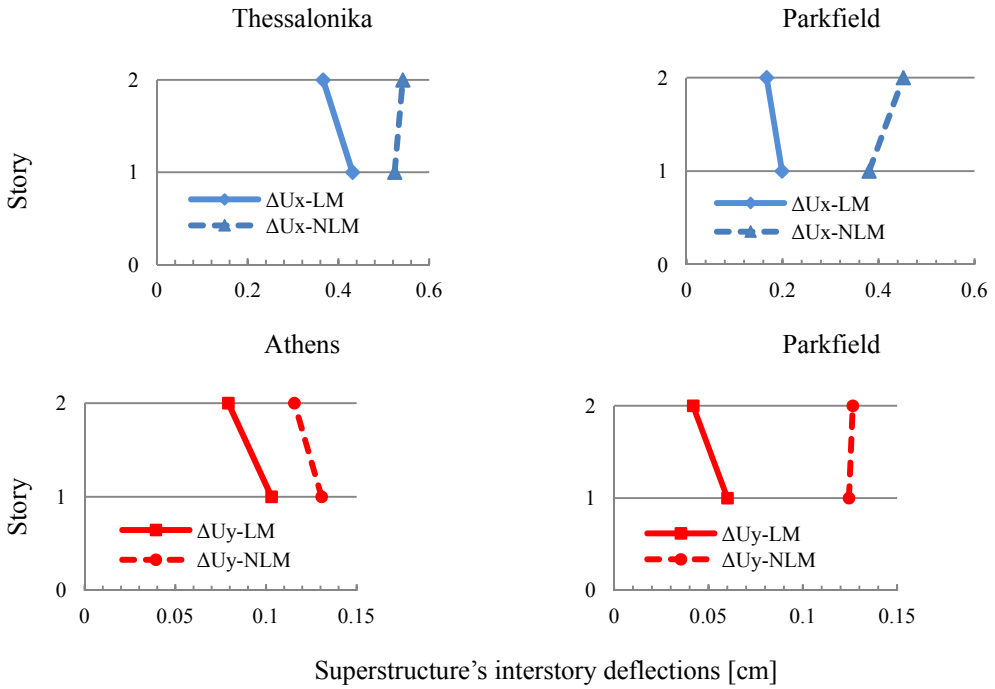

Fig. 11 Superstrusture's interstory deflections under earthquake excitations that generate moderate structural response, along the *X* and *Y* directions under the EC_1 and EC_2 combinations, respectively

Moreover, Fig. 12(a) shows that the linear model exhibits minor relative errors on the computation of the maximum absolute accelerations of the seismic isolation diaphragm and the 1st story along the *X* direction. Contrarily, it leads to a significant non conservative underestimation of 27.8 % of the second story's absolute acceleration, while an overestimation of the respective accelerations is noticed along the *Y* direction (Fig. 12(a)). A similar error of approximately -15.0 % is noted at the isolation diaphragm and the 1st story's accelerations, while the error is reduced to -13.2 % at the 2nd story. Another important observation is that the linearized model, under various excitations, yields an approximately orthogonal height distribution of accelerations, which is altered by the nonlinear model (Fig. 13), probably due to the excitation of higher eigenmodes, which is a phenomenon that the linear model cannot capture.

The linear analyses exhibit an overestimation of the maximum base shear forces, 2.3 % along the *X* direction and 11.9 % greater along the transverse direction (Fig. 12(b)). Story shear forces are significantly non-conservatively underestimated along the *X* direction and the relative error is increased by height, specifically, by 11.8 % at the 1st and 25.7 % at the 2nd story. On the contrary, story shear forces are overestimated along the *Y* direction and the relative error is not fluctuating much by height, since it is equal to -12.3 and –11.6 % at the 1st and 2nd story, respectively. The

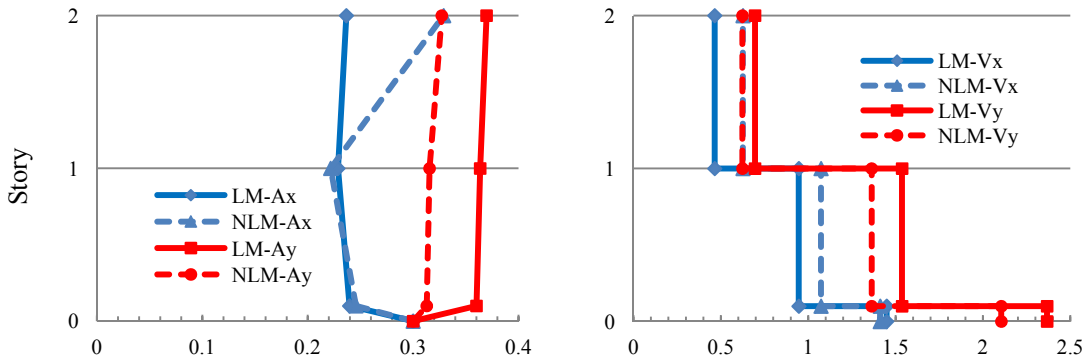

(a) Absolute accelerations [g] (b) Shear forces [MN]

Fig. 12 Envelope of: (a) maximum absolute floor accelerations and (b) maximum floor shear forces, of the SIS, along the *X* and *Y* directions under the EC_1 and EC_2 combinations, respectively

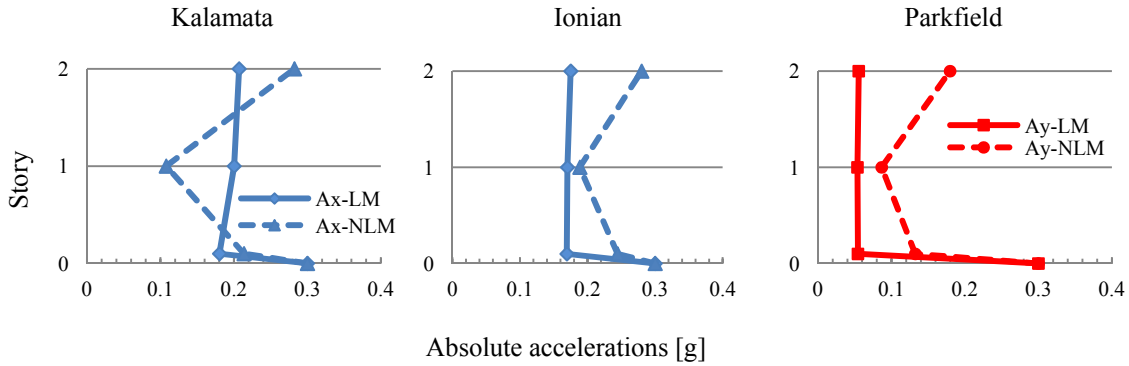

Fig. 13 Absolute accelerations under earthquake records that excite higher eigenmodes

heterogeneous errors in the estimation of the shear forces along the two principal horizontal directions indicate that the characteristics of the superstructure and the frequency content of the earthquake excitations have an effect on the accuracy of the linear model. Moreover, the linear model is considered unsuitable for the design of the superstructure due to the substantial underestimation of the story shear forces along the *X* direction.

It can be concluded from the computed results that the linearization of the LRBs' constitutive law yields a relatively accurate model of the response of the isolation system under excitations with equal PGA with the DBE, but not under higher magnitude earthquakes, as it is shown in the next section. The detailed modeling of the LRBs' nonlinear behavior and their hysteretic energy dissipation mechanism, by the adoption of Bouc-Wen model, alters noticeably the response of the superstructure. The usage of the linearized model leads to an overestimation of the SIS' response along the *Y* direction and an underestimation along the *X* direction. It is evident that in order to obtain an adequately accurate analysis and design of a SIS, isolated partially or entirely with LRBs, the nonlinear behavior of the seismic isolation system should be explicitly modeled.

6. Determination of the size of the seismic gap

The displacements of the isolation system beyond the excitations with equal PGA with the DBE, are calculated for two higher levels of earthquake magnitude. The relative error of the isolation system's displacements, due to the linearization of the LRBs' properties is derived parametrically with the PGA. Furthermore, these displacements are compared with the width of the seismic gap, which has been determined according to the methodologies of Eurocode 8 and UBC 1997, for 3 levels of earthquake's PGA (Table 5). Under higher magnitude earthquakes than the DBE, the effective stiffness of the isolation system decreases, which results in an increase of the energy that is dissipated by the isolation system through loading, unloading and reloading cycles. However, its equivalent viscous damping ratio $\xi_{effisol}$ is reduced due to the significant decrease of the ξ_{eff} of the LRBs.

It is evident from Fig. 14 that the linearized model provides an adequately accurate estimation of the maximum displacements of the seismic isolation system along the *X* direction, regardless of the PGA. When the intensity of the excitations and the respective responses of the structure attenuate, the linearized model leads to an overestimation of the relative displacements of the isolation system, in the time range between 20 and 60 seconds. Under these circumstances, the effective stiffness of the isolators is less than their actual stiffness, explaining the development of higher displacements. Also, Fig. 14 indicates that Eurocode 8 and UBC 1997 provide a sufficiently

Table 5 Violations of the provided seismic gap while using linear and nonlinear models

	Maximum percentage exceedance :					
	Eurocode 8			UBC 1997		
PGA	Gap (cm)	LM	NLM	Gap (cm)	LM	NLM
0.30 g	10.76	25.8 %	26.2%	9.31	45.4 %	45.9%
0.40 g	16.24	34.5 %	24.9 %	14.15	54.4 %	43.3 %
0.50 g	22.49	40.6 %	20.6 %	19.67	60.7 %	37.9 %

wide seismic gap (red and green horizontal lines, respectively), in order to avoid collision incidents to the restraining moat wall. On the other hand, the usage of the linearized model leads to an overestimation of the maximum displacements of the isolation system along the *Y* direction, for all studied levels of PGA. The provided clearance is violated significantly, whether is calculated according to the provisions of Eurocode 8 or UBC 1997. Specifically, the envelope time histories of both models exceed twice Eurocode 8. Linear analyses demonstrate 3 discrete violations of the UBC's 1997 gap, while nonlinear analyses exhibit 2 violations.

The maximum relative displacements of the seismic isolation system along the two principal directions and the calculated sizes of the seismic gap are presented in Fig. 15. It is obvious that Eurocode 8 yields greater total displacements, since the displacements are multiplied with a magnification factor equal to 1.2, although the additional displacements due to accidental torsion are less. The methodologies of both design codes provide a secure estimation of the relative

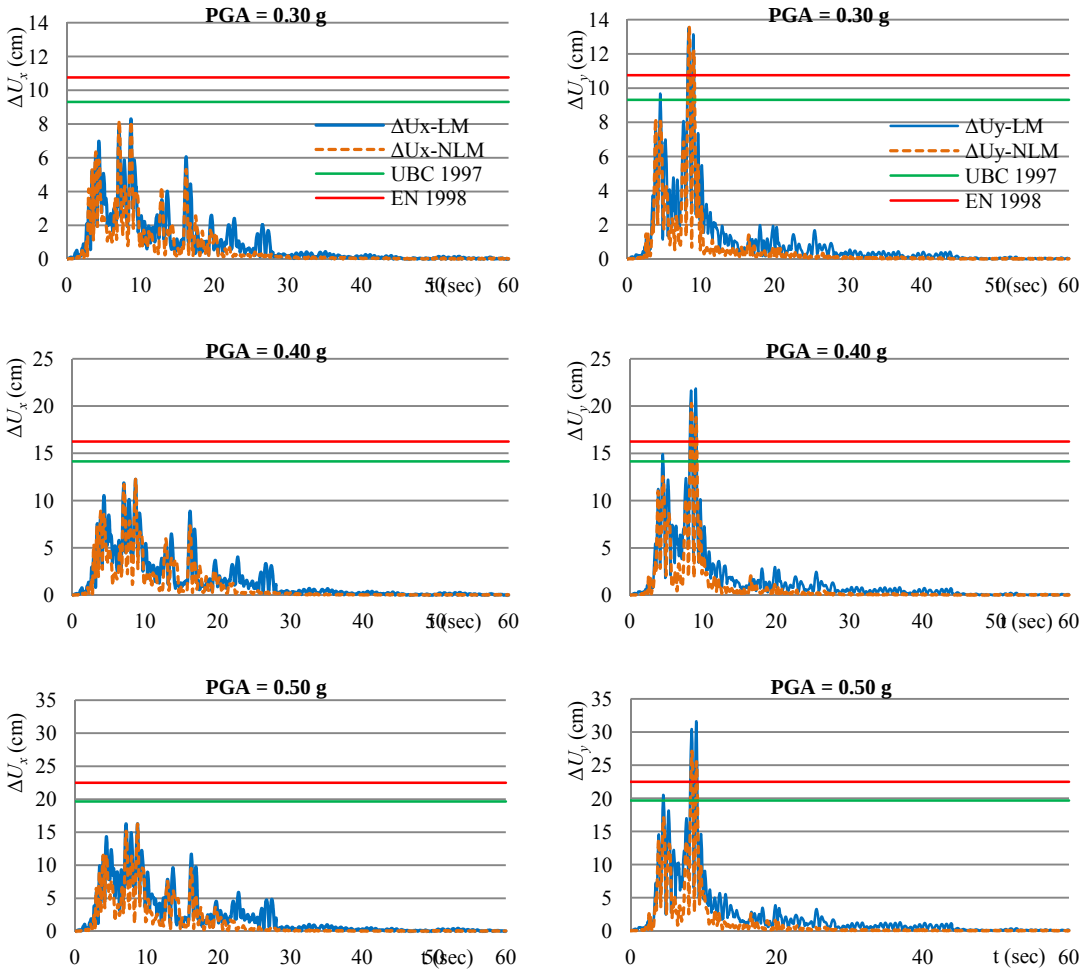

Fig. 14 Envelope time history of absolute maximum relative displacements of the isolation system, along the *X* and *Y* directions under the EC_1 and EC_2 combinations, respectively

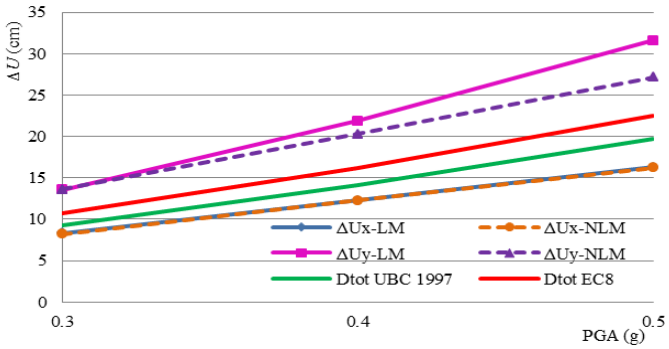

Fig. 15 Maximum relative displacements of the isolation system along the *X* and *Y* directions *vs*. PGA

displacements along the *X* direction, but they yield insecure results in the *Y* direction. As the earthquake magnitude increases, the linearized model provides better estimations of the maximum displacements of the isolation system along the *X* direction, but overestimates further the displacements along the *Y* direction with the overestimation error rising with the increase of the earthquake's PGA. It is demonstrated that the considered methodologies are approximate and can only be used for the preliminary estimation of the required width of the clearance. Nonlinear analysis is necessary for the determination of the required width of the seismic gap in order to prevent the catastrophic effects of potential structural collision to the surrounding moat wall, without unnecessary waste of valuable space.

7. Superstructure's inelastic deformations

7.1 Alteration of the structural response

The superstructure of the seismically isolated building undergoes inelastic deformations only when the principal seismic component acts along the *Y* direction (EC2), under excitations with higher earthquake excitation than the DBE. When the principal seismic component is imposed along the *X* direction (EC1), all members of the superstructure respond within the elastic range, regardless of the value of the PGA. Under the action of the Kocaeli excitation along the *Y* direction, scaled to a 0.40 g PGA, all 1st story braces yield due to axial buckling. The developed inelastic deformations have negligible effect on the maximum displacement of the isolation system along the respective direction. However, as it can be observed in Fig. 16, the ENLM presents a slight increase (0.9 %) in the 1st story's maximum relative displacement due to the reduction of the stiffness of the respective level, while the 2nd story's maximum relative displacement decreases by 0.9 %. Under a PGA of 0.50 g, all 1st story's braces yield due to axial buckling and develop substantially more intensive inelastic response than under a PGA of 0.40 g. While the alteration of the maximum displacement of the isolation system is insignificant, the 1st story's maximum relative displacement increases by 6.3 % (Fig. 16), due to the more extensive reduction of the stiffness of the particular story, and the maximum relative displacement of the 2nd story is slightly reduced, by 0.4 %. Therefore, the inelastic deformations that are developed at the 1st story amplify

the maximum relative displacement at the specific level with the increase of the PGA of the imposed excitations, while the maximum relative displacement of the upper story is slightly reduced, having negligible influence on the maximum relative displacement of the isolation system.

At the 1st story, the level where inelastic deformations take place, the shift of the maximum absolute acceleration is negligible, regardless the PGA of the imposed excitations, as shown in Fig. 17. However, a slight decrease of the lower and upper diaphragms' maximum absolute acceleration occurs. Specifically, maximum absolute acceleration of the isolation's diaphragm is reduced by 0.5 and 0.8 %, under PGA of 0.40 and 0.50 g, respectively. The corresponding reductions on the 2nd story's diaphragm are equal to 1.1 and 0.8 %. Contrarily with the determination of the maximum interstory deflections, the nonlinear model provides an accurate estimation of the maximum absolute accelerations of the structure for the particular problem.

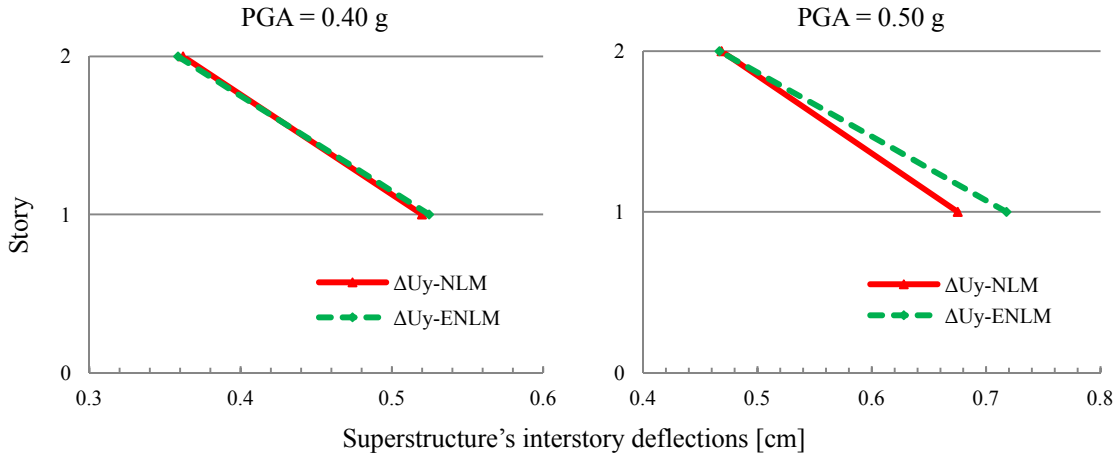

Fig. 16 Superstrusture's maximum interstory deflections along the *Y* direction, under the EC_2 combination

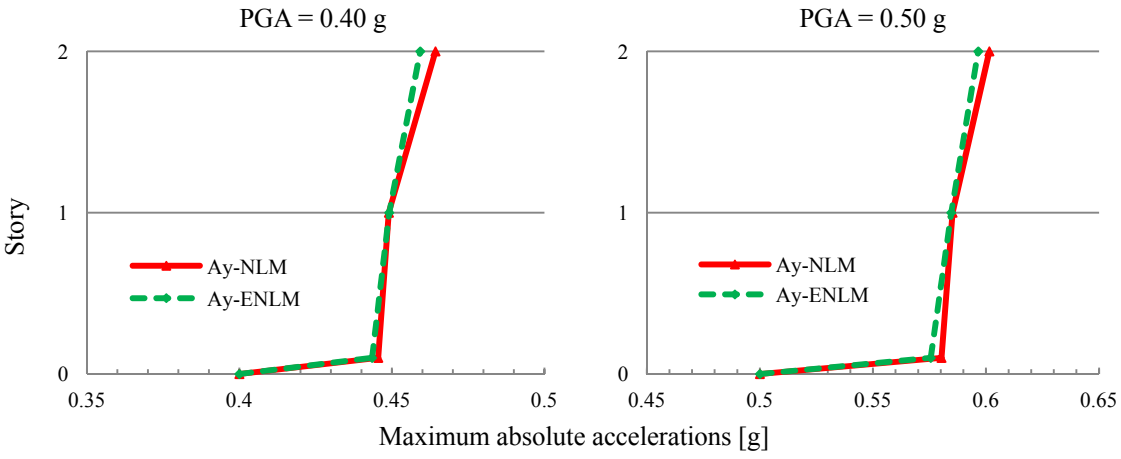

Fig. 17 Maximum absolute accelerations along the *Y* direction, under the EC_2 combination

As it is observed in Fig. 18 the effect of the inelastic deformations of the superstructure on the base shear force is insignificant, regardless of the PGA of the earthquake excitation, due to the negligible alteration of the maximum displacement of the isolation systems. The 1st story's shear force along the *Y* direction is decreased by 1.6 and 1.4 %, under a PGA equal to 0.40 and 0.50 g, respectively, while greater percentage decrease is observed to the 2nd story's shear force, where the corresponding reductions equal 4.1 and 3.9 %, respectively.

It is concluded that the superstructure of the base isolated building can develop inelastic deformations, if it is subjected to excitations higher than the DBE. The inelastic deformations affect the superstructure's response, but as they don't have substantial influence on the response of the isolation system, due to the fact that the latter is dominated by a higher damping capacity and that the inelastic deformations of the superstructure are limited. In the case under consideration, the shift of the superstructure's response is small, since the inelastic deformations are limited at the 1st story's braces and not to any other structural elements. These braces yield under compressive load, due to axial buckling, which is a rather brittle mode of yielding with a low energy dissipation capacity. It should be noted that the inelastic deformations of the superstructure might be even more influential in structures with different yield mechanisms. Therefore, the inelastic behavior of the superstructure should be explicitly modeled, especially when the response of the building under high earthquake excitations is investigated.

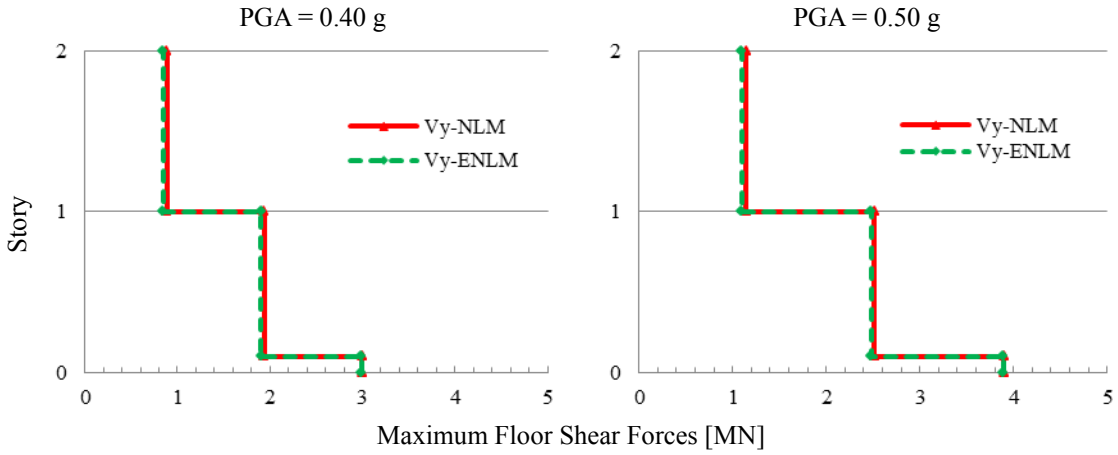

Fig. 18 Maximum floor shear forces along the *Y* direction, under EC_2 combination

7.2 Structural failures

The comparison of the structural failures that arise from the analyses of the three models, the linearized (LM), the nonlinear (NLM) and the extended nonlinear model (ENLM), is considered essential. Any exceedance of the yield limit is considered structural failure for the ENLM, while any exceedance of the members' resistance design values, as they have been calculated according to the provisions of Eurocode 3, is considered as failure for the LM and the NLM. All three models respond elastically under excitations with PGA equal to the DBE. Under the selected earthquakes scaled to a 0.40 g PGA, the analyses using the LM demonstrate failure of all braces and eight

columns of the 1st story (Fig. 19). The failure mechanism of the braces is axial buckling, while the columns are damaged due to biaxial moment and axial force interaction. The analyses of the NLM and the ENLM limit the failures at the 8 braces of the 1st story, whereas all the columns remain elastic. If the LM model is analyzed, all of the 1st story columns and braces and half of the 2nd story braces fail under excitations with a PGA equal to 0.50 g. The usage of the NLM limits the exhibited failures to all braces and 14 columns of the 1st story, while the analyses using the ENLM indicate only yielding of the 1st story braces due to axial buckling. The latter demonstrates an important advantage of utilizing seismic isolation for the particular building; that even under earthquakes, significantly more severe than the DBE, the vertical load resisting system of the building remains undamaged. The rehabilitation cost, which corresponds to the replacement to the 1st story braces, is relatively low and the repairing tasks do not necessitate the evacuation of the building as they can be executed without any temporary support measures.

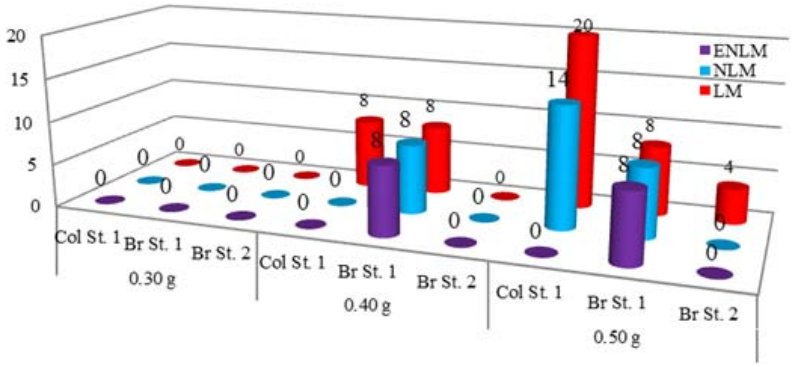

Fig. 19 Failures of superstructure's members under 3 levels of the PGA, while using extended nonlinear (ENLM), nonlinear (NLM) and linearized models (LM)

The adoption of the Bouc-Wen constitutive law for the modeling of the shear behavior of the LRBs decreases the number of structural failures. Earthquakes with strong low frequency content, such as the applied Kocaeli and Northridge excitations, generate "excessive" translational response of the isolation system and lead to structural failures. Under this category of excitations, where the actual displacement of the isolation system exceeds the targeted or the design displacement, the linear analyses indicate increased number of structural failures due to underestimation of the damping provided by the LRBs. Therefore, the explicit modeling of the hysteretic energy dissipation mechanism of the LRBs, in combination with the further shifts of the structure's fundamental eigenperiods limits the structural failures. The analytical modeling of the inelastic behavior of the superstructure's elements results in further reduction of their failures. In the particular problem, it is observed that the failures are limited only at the 1st story braces without any column undergoing inelastic deformations. This phenomenon occurred due to two reasons. Firstly, the explicitly modeled hysteretic energy dissipation mechanism of the braces due to axial loading contributes to the avoidance of the development of inelastic deformations to other structural members. Secondly, the implementation of fiber elements enables the more accurate determination of the columns' internal forces. The failures of some columns that are detected in the models with linear elastic superstructure are not actual failures but inadequacies of the members to

fulfill the approximate condition of Eurocode 3 for the biaxial moment and axial force interaction. The assumption of linear elastic behavior for the superstructure is proved conservative regarding the determination of the structural failures and it can be used only for the preliminary design of the structural elements. The consideration of the inelastic behavior of superstructure's members is necessary for a detail detection of structural failures and beneficial for the accuracy of the structural design and optimization.

8. Effect of superstructure's inelasticity during collision incidents to the restraining moat wall

The response of the SIS is strongly amplified when a collision with the adjacent moat wall occurs with a dramatic increase of the interstory deflections due to the impact energy that is induced in the building. The relative displacements at the base isolation level are reduced because of the kinematic barrier that the moat wall imposes, while the acceleration response of the structure rises substantially. Regarding the considered seismic combinations, a minor change of the isolation system displacements is detected (Fig. 20). The usage of the NLM does not significantly affect the estimation of the maximum relative displacements of the isolation system along the X and Y directions, while more significant discrepancies are noted at the interstory deflections of the structure (Fig. 21). The implementation of the NLM yields overestimation errors of the 1st and 2nd floor interstory deflections along the X direction, with the maximum errors occurring under the Kocaeli pair of excitations and with a general trend of the error to increase with height. Overestimation errors of the maximum interstory deflections are also recorded along the Y direction, reaching maximum values under the Kalamata pair of excitations (12.9 and 11.5 % at the 1st and 2nd story, respectively).

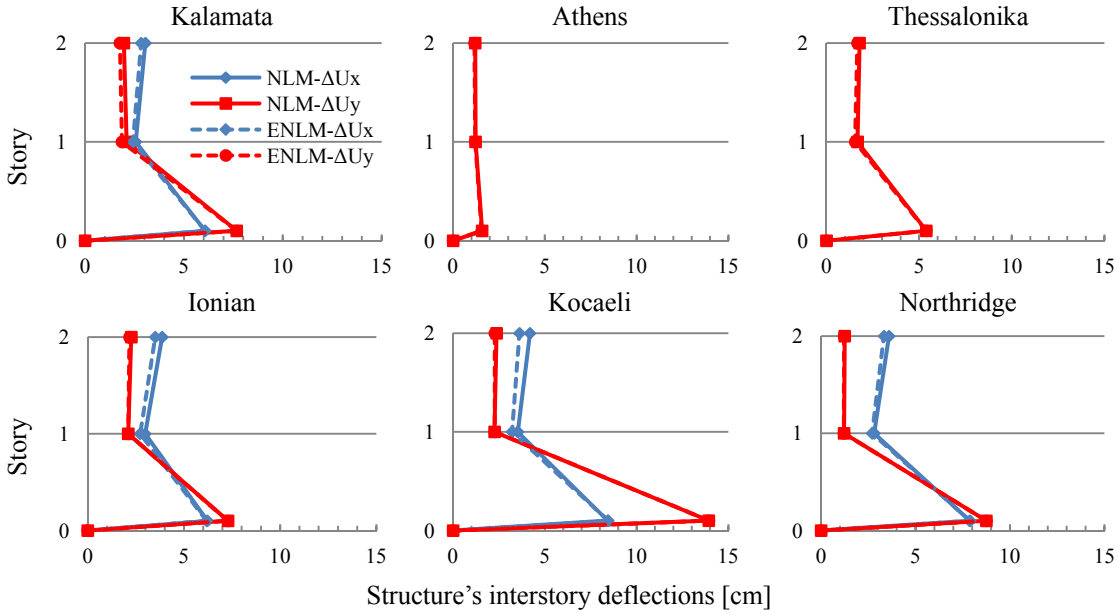

Fig. 20 Alteration of interstory deflections due to inelastic deformations of the superstructure

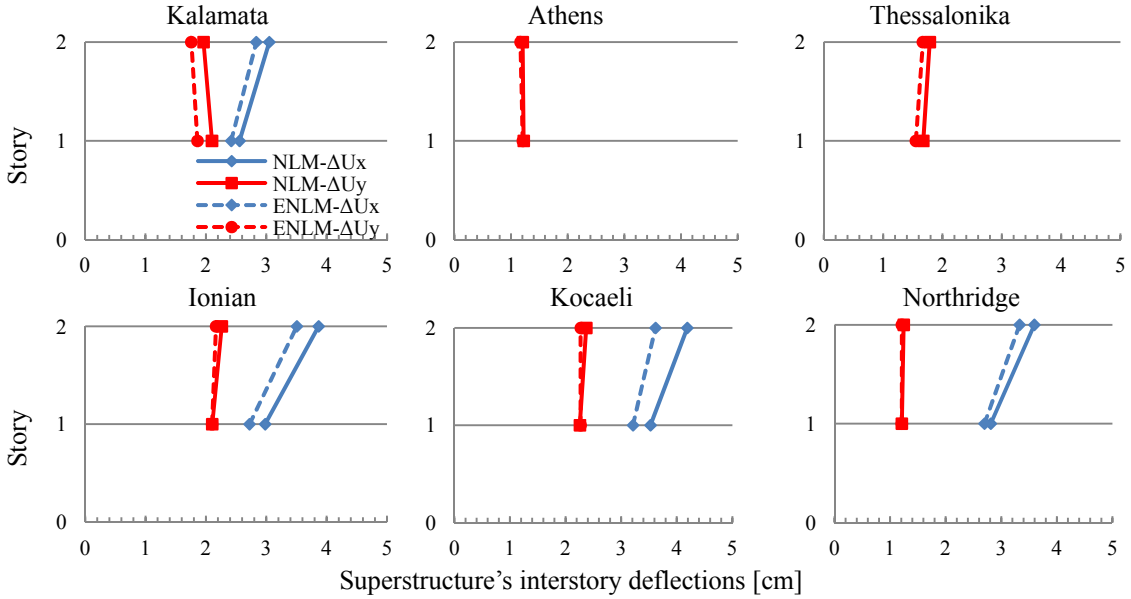

Fig. 21 Alteration of superstructure's interstory deflections due to inelastic deformations of the superstructure

Regarding the acceleration response, Fig. 22 indicates that the inelastic deformations of the superstructure affect the maximum absolute accelerations at the isolation diaphragm. Dispersion of the errors is ascertained with the NLM analyses along the *X* direction, where the maximum overestimation is 13.5 % (Ionian pair of excitations) and the maximum underestimation is 6.3 %

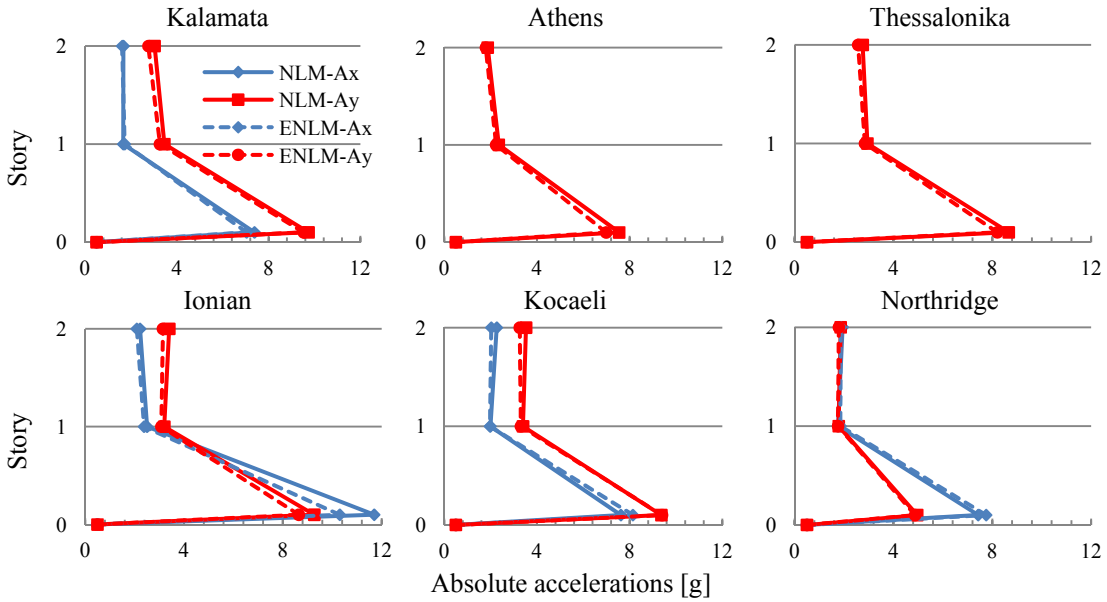

Fig. 22 Alteration of absolute floor accelerations due to inelastic deformations of the superstructure

(Kocaeli pair of excitations). The maximum overestimation error along the *Y* direction (8.0 %) is recorded under the Athens pair of excitations, while the maximum underestimation error is only 0.3 % (Kocaeli pair of excitations). The maximum errors are reduced on the 1st story diaphragm. Along the *X* direction the maximum underestimation error is 5.3 %, whereas the maximum overestimation error is 5.1 %. The maximum overestimation error along the transverse direction is 6.0 % and no underestimations have been noted. The discrepancies rise at the 2nd story diaphragm, where only overpredictions of the acceleration are noticed. The maximum underestimation error is equal to 11.7 and 9.7 %, along the *X* and *Y* directions, respectively.

It is concluded that the inelasticity of the superstructure affects the response of the SIS when experiencing structural collision to the surrounding moat wall. In general, the inelastic deformations developed by the elements of the superstructure lead to reductions of the structural response. During collisions with the moat wall, the structure undergoes extended inelastic deformations, which reduce significantly the stiffness of the superstructure. This stiffness reduction results in the instantaneous elongation of the fundamental periods of the superstructure, which reduces the seismic induced actions. Furthermore, the inelastic deformations of the structural members are directly related to the increase of the energy that is dissipated hysteretically by the system, which results in a reduction of the response of the superstructure. In many of the studied combinations, the structure experiences more than one collision incidents, due to the narrow seismic gap and the high magnitude of the excitations, which increases the amount of hysteretically dissipated energy, leading to further variation of the results obtained from the NLM and ENLM analyses. In the few cases that the ENLM develops higher acceleration response, that happens probably due to an excitation of higher eigenmodes or due to an amplification of their contribution in the overall structural behavior. Since, the discrepancies between the NLM and the ENLM are not negligible, the inelasticity of the superstructure should be taken into account while considering structural collision incidents of seismically isolated buildings against the surrounding moat wall.

9. Conclusions

The linearization of the shear behavior of the LRBs may result in significant errors in the computation of the structural response of a base isolated building. The frequency content and the intensity of the imposed excitations as well as the stiffness of the superstructure have a strong influence on the inaccuracy of the linearized model. Significant dispersion of the relative errors in the computed maximum interstory deflections and absolute floor accelerations is evident, since underestimation and overestimation errors arise along the two principal horizontal directions. In addition, the analyses of the linear model lead to non-conservatively underestimated interstory deflections, especially under earthquake excitations that cause moderate response of the seismic isolation system. The discrepancies in the height distribution of the absolute floor accelerations indicate a major inadequacy of the linearization approach, thus the inability in capturing phenomena of excitation or amplification of the contribution of the higher eigenmodes. The usage of a linearized model shall be restricted in the preliminary analysis phase, since it yields, in some cases, insecurely underestimated results. The implementation of the Bouc-Wen model is considered necessary for both analysis and design of a seismically isolated building. Furthermore, nonlinear analyses should be performed for the accurate calculation of the required width of the seismic gap, since methodologies for its calculation, provided by the Eurocode 8 and the UBC 1997, are very approximate. Since, the considered building is a typical low-rise structure, the accuracy of these

two issues, specifically the linearization approach and the methodology for the calculation of the required width of the seismic gap, can been argued for many similar structures and their reconsideration, in a future revision of Eurocode 8, is strongly recommended. Therefore, it is strongly recommended that the analysis and design of unconventional earthquake resistant structures, such as base isolated buildings, should not be based solely on the provisions of the design codes. The engineers' judgment is essential and should be applied in the critical filtering of these provisions and the establishment of adjunctive measures in order to achieve the optimum structural performance of such buildings.

The analyses have revealed that the inelasticity of the superstructure of a seismically isolated building should be taken into account, especially, if its response, under excitations with higher PGA than the DBE, is investigated. A limited amplification of the maximum interstory deflections occurs at the story where inelastic deformations are developed, as a result of the decrease of the stiffness of the particular story. The degree of the particular amplification is directly related to the PGA of the imposed excitation. Beyond the direct effect on the superstructure's response, the analyses of the extended nonlinear model provide a more accurate determination of the internal forces and the deformations of the structural members, which can be utilized in the optimization of the superstructure.

Furthermore, it has been shown that the consideration of the inelasticity of the superstructure results in a substantial modification of the response of a seismically isolated building when structural collision incidents to the surrounding moat wall occur. The inelastic deformations of the superstructure lead to an attenuation of the superstructure's response, mainly due to the sudden shift of the fundamental periods of the structure and the hysteretic energy dissipation mechanism provided by the inelastic deformations of the structural members of the superstructure.

References

Bouc, R. (1967), "Forced vibration of mechanical systems with hysteresis", *Proceedings of the Fourth Conference on Nonlinear Oscillation*. Prague, Czechoslovakia, September.

Cardone, D., Flora, A. and Gesualdi, G. (2011), "Inelastic response of seismically isolated structures", *Proceedings of the 12th World Conference on Seismic Isolation Energy Dissipation and Active Vibration Control of Structures*, Sochi, Russia, September.

Charalampakis, A.E. and Koumousis, V.K. (2008), "On the response and dissipated energy of Bouc Wen hysteretic model", *J. Sound Vib.*, **309**, 887-895.

Chen, B.J., Tsai, C.S. and Chung, L.L. (2006), "Seismic behavior of structures isolation with a hybrid system of rubber bearings", *Struct. Eng. Mech.*, **22**(6), 761-783.

Computers and Structures Inc. (2010), *CSI Analysis Reference Manual for SAP2000, ETABS, and SAFE*, Berkeley, California, USA.

Dicleli, M. and Buddaram, S. (2007), "Comprehensive evaluation of equivalent linear analysis method for seismic-isolated structures represented by sdof systems", *J. Eng. Struct.*, **29**, 1653-1663.

Elnashai, A.S. and Di Sarno, L. (2008), *Fundamentals of earthquake engineering*, John Wiley & Sons Ltd., West Sussex, UK.

European Committee for Standardization (2009), *EN 15129:2009*, *Anti-seismic devices*, Brussels, Belgium.

European Committee for Standardization (2005), *EN 1993-1-1:2005*, *Eurocode 3: Design of steel structures - Part 1-1: General rules and rules for buildings*, Brussels, Belgium.

European Committee for Standardization (2004), *EN 1998-1:2004*, *Eurocode 8: Design of structures for earthquake resistance - Part 1: General rules, seismic actions and rules for buildings*, Brussels, Belgium.

Federal Emergency Management Agency & Virginia: American Society of Civil Engineers, FEMA 356 (2000), *Prestandard and commentary for the seismic rehabilitation of buildings*,Washington, D.C., USA.

Higashino, M. and Okamoto, S. (2006), *Response control and seismic isolation of buildings*, Taylor & Francis, Oxon, UK.

Iwan, W.D. and Gates, N.C. (1979), "The effective period and damping of a class of hysteretic structures", *Earthq. Eng.Struct. Dyn.*, **7**, 199-211.

Kelly, T.E. (2001), *Base isolation of structures*. *Design Guidelines*, Holmes Consulting Group, Wellington, New Zealand.

Kilar, V. and Koren, D. (2009), "Seismic behaviour of asymmetric base isolated structures with various distributions of isolators", *Eng. Struct.*, **31**, 910-921.

Kilar, V. and Koren, D. (2010), "Simplified inelastic seismic analysis of base-isolated structures using the N2 method", *Earthq. Eng.Struct. Dyn.*, **39**, 967-989.

Komodromos, P. (2000), *Seismic isolation for earthquake resistant structures*, WIT Press, Southampton, UK.

Mahmoud, S. and Jankowski, R. (2010), "Pounding-involved response of isolated and non-isolated buildings under earthquake excitation", *Earthq. Struct.*, **1**(3), 231-252.

Makris, N. and Kampas, G. (2013), "The engineering merit of the "Effective Period" of bilinear isolation systems", *Earthq. Struct.*, **4**(4), 397-428.

Matsagar, V.A. and Jangid, R.S. (2004), "Influence of isolator characteristics on the response of base isolated structures", *Eng. Struct.*, **26**, 1735-1749.

Mavronicola, E. and Komodromos, P. (2011), "Assessing the suitability of equivalent linear elastic analysis of seismically isolated multi-storey buildings", *Comput. Struct.*, **89**, 1920-1931.

Naeim, F. and Kelly, J.M. (1999), *Design of seismic isolated structures*, *From theory to practice*, John Wiley & Sons Inc., Hoboken, NJ, USA.

Nagarajaiah, S., Reinhorn, A.M. and Constantinou, M.C. (1991). "Nonlinear dynamic analysis of 3-D-base isolated structures", *J. Struct. Eng.*, **117**(7), 2035-2054.

Pant, D.R. and Wijeyewickrema, A.C. (2012), "Structural performance of a base-isolated reinforced concrete building subjected to seismic pounding", *Earthq. Eng.Struct. Dyn.*, **41**, 1709-1716.

Park, Y.J., Wen, Y.K. and Ang, A.H.S. (1986), "Random vibration of hysteretic systems under bidirectional ground motions", *Earthq. Eng.Struct. Dyn.*,, **14**, 543-557.

Polycarpou, P.C. and Komodromos, P. (2011), "Numerical investigation of potential mitigation measures for poundings of seismically isolated buildings", *Earthq. Struct.*, **2**(1), 1-24.

Powel, H.G. (2010), *Modeling for structural analysis. Behavior and basics*, Computers and Structures Inc., Berkeley, California, USA.

Providakis, C.P. (2008), "Pushover analysis of base-isolated steel–concrete composite structures under near-fault excitations", *Soil Dyn. Earthq. Eng.*, **28**, 293-304.

Qiang, Y., Li, Z. and Xinming, W. (2010), "Parameter identification of hysteretic model of rubber-bearing based on sequential nonlinear least-square estimation", *Earthq. Eng.Eng. Vib.*, **9**(3), 375-383.

Skinner, R.I., Robinson, W.H. and McVerry, G.H. (1993), *An introduction to seismic isolation*, John Wiley & Sons Ltd, West Sussex, UK.

Tena-Colunga, A. and Escamilla-Cruz, J.L. (2007), "Torsional amplifications in asymmetric base isolated structures", *Eng. Struct.*, **29**, 237-247.

Tsai, H.C. (1997), "Dynamic analysis of base-isolated shear beams bumping against stops", *Earthq. Eng.Struct. Dyn.*, **26**, 515-528.

International Conference of Building Officials, Uniform Building Code (1997), *Structural engineering design provisions*, California, USA.

Wen, Y.K. (1976), "Method for random vibration of hysteretic systems", *J. Eng. Mech. – ASCE*, **102**(2), 249-263.

Wu, C., Li, Y., Li, H. and Zhang, K. (2008), "Parametric study on seismic energy response of base-isolated structures", *International Workshop on Modelling, Simulation and Optimization,WMSO 2008*, Hong Kong, China, December.

SA